Neuroscience Informatics 2 (2022) 100015

Contents lists available at ScienceDirect

Neuroscience Informatics

www.elsevier.com/locate/neuri

NaaS

Engineering technology characterization of source solution for ZnO and their data analytics effect with aloe vera extract

Neha Verma [a,*], Manik Rakhra [b], Mohammed Wasim Bhatt [c], Urvashi Garg [d]

[a] Department of Physics, KRM DAVcollege Nakodar, India
[b] Department of Computer Science and Engineering, Lovely Professional University Phagwara, India
[c] Department of Computer Science and Engineering, Central University of Punjab, India
[d] Department of Computer Science and Engineering, Chandigarh University, Punjab, India

ARTICLE INFO

Article history:
Received 12 September 2021
Received in revised form 2 October 2021
Accepted 7 October 2021

Keywords:
ZnO nanomaterials
Neuroscience
Engineering technology
XRD
FESEM
FTIR
LCR meter

ABSTRACT

Increased population has led to create the environmental related issues. Zinc Oxide has great attention due to its application in versatile smart and functional material. In the recent paper, we have observed the variation in shape and size for different precursor (0.45 M - Zn acetate dihydrate, Zn nitrate hexahydrate) with aloe vera extract ZnO nanoparticles, data analytics have been prepared with annealing at 650 °C. The prepared solution was analyzed by using simple solution method. Structural, morphological, optical and electrical properties defined certain nanomaterials. XRD spectra showed polycrystalline in nature. In the case of Zn nitrate, more instance peaks are found and SEM reveals the particle size drop into a range of 50-90 nm. Analysis of FTIR was conducted to classify the mineral constituents. The further capacitance levels are measured at a low scale. The resistivity spectrum of ZnO nanoparticles ranged from 3×10^{-2} to 5×10^{-2} (in cm)$^{-1}$. Optical band gap of the synthesized particles lies in the range of 3.10-3.20 eV, which confirmed that nanoparticles are suitable for gas sensor and solar cell applications. These synthesized nanoparticles can further be used for the neuroscience application such as fabrication of medical instruments and for medical purpose too. In turn, these materials contribute to novel diagnostic and therapeutic strategies, including drug delivery, neuroprotection, neural regeneration, neuroimaging and neurosurgery.

1. Introduction

It is a semi conductive unit with a band gap of 3.37 eV and a high exciton binding energy of 60 MeV at room temperature, like a small number of other products like GaN with a 3.4 eV band gap and a binding energy of 21 MeV. Such features offer a good basis for ZnO in producing optoelectronic products such as LED [1], laser system [2], field emission transistor [3] and drug delivery. It has an oxygen vacancy function, so it is useful in the manufacture of sensors for oxygen gas [4]. ZnO nanoparticles have been researched in diverse applications and in the medical field. Materials are added strongly based on form and scale. To monitor these, various variables such as pH, concentration, dopant, solvents, ageing period must be varied with the usage of specific physical and chemical techniques [5–11]. Specific heat management approaches within these strategies provide many benefits over others in terms of low cost and flexibility in process operation.

Aloe vera is a succulent, plant-like cactus that grows in a warm, hot environment, and aloe vera gel includes vitamins A, C, and E. A. and Ayeshamariam [12] reported biosynthesis and antibacterial analyses of the nanocomposites. E has researched green synthesis of the ZnO nanoparticles. Varghese [13]. Jeeva lakshmi V et al. [14] observed Biotechnical synthesis of nanoparticles is effective as synthesized with the use of Aloe Vera by chemical method.

A number of researchers have studied that the ZnO should be doped with different dopants such as In, Al, Sn, Sb and Ni to improve optoelectronic properties and surface defects [15,16]. Some of the scientists covered the effects of rare terrestrial elements as active dopants on ZnO interstitial sites, which can help to reduce the electron-hole combination, which is the precondition for gas sensing and photodegradation of colors [17]. Research is surrounding around for the fabrication of smart and functional devices, therefore for creation of these devices it is important to control the different structural, optical, morphological, thermal, sensing and photocatalytic properties.

* Corresponding author.
E-mail addresses: nv0027@gmail.com (N. Verma), Rakhramanik786@gmail.com (M. Rakhra), wasimmohammad71@gmail.com (M.W. Bhatt), urvashi.mittal80@gmail.com (U. Garg).

https://doi.org/10.1016/j.neuri.2021.100015

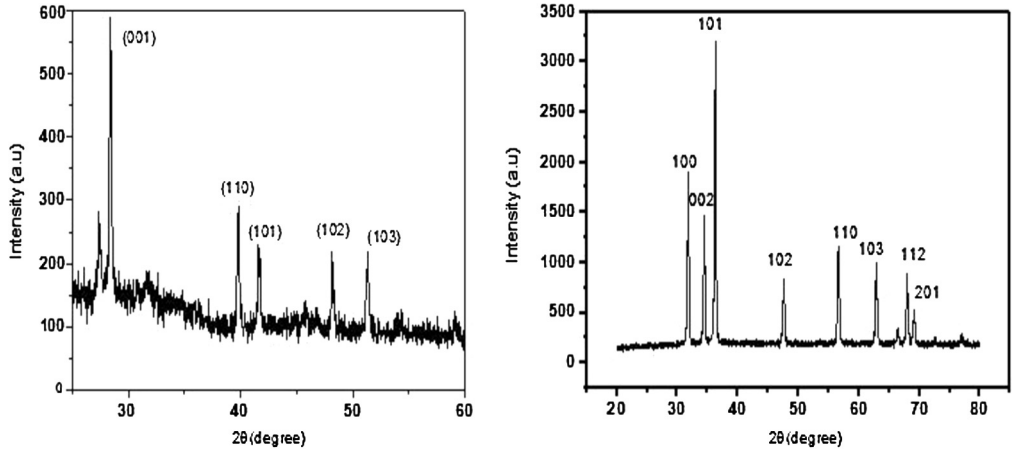

Fig. 1. XRD spectra of ZnO nanoparticles (a) Zn acetate dehydrate (b) Zn nitrate hexahydrate.

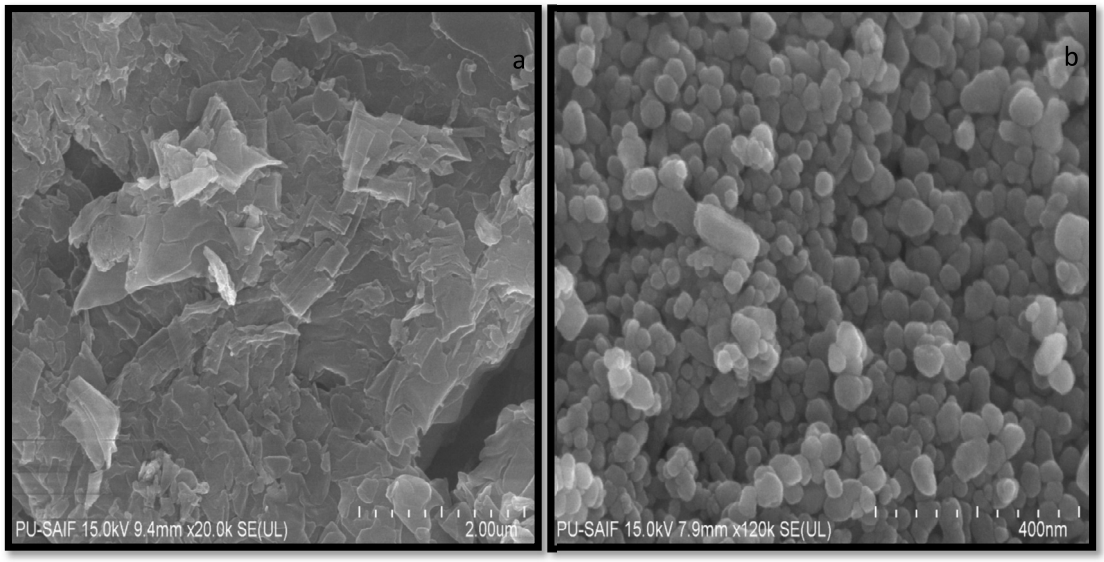

Fig. 2. ZnO particles (a) Zn dihydrate acetate (b) hexahydrate Zn nitrate pictures in FESEM.

In this study, the authors synthesize ZnO nanoparticles by using separate source solution and Aloe vera plant using simple heat treatment process. No existing literature has been studied, to the best of our knowledge, the influence of various precursors on ZnO nanoparticles and contrasted with electrical properties.

2. Experimental details

2.1. Synthesis of ZnO nanoparticles with extract aloe vera

ZnO nanoparticles were synthesized using a basic heat treatment process. For this reaction phase Zn nitrate hexahydrate and Zn acetate dihydrate is the maternal solution for the samples. In the synthesis method, 10 ml of aqueous solution of 0.45 M Zn acetate and Zn nitrate was combined with 0.02 M of glucose (10 ml) as fuel in deionized water as a solvent. The combined solution was stirred for 30 min with magnetic stirrer at 80 °C, eventually achieving homogeneous solution. Aloe vera leaves gathered from botanical garden and vigorously washed using deionized water and squeezed the inner gel from the skin, poured this gel into the formulated solution, stirred again for 30 minutes. Until the synthesized mixture was mixed, filtered with whatman filter paper (No. 1) and sent to the crucible, placed in the muffle furnace at 550 °C for 10-20 min. Spongy like substance is produced during heating phase. Then ring it again at 650 °C for 40 min. White powder was eventually collected, and their optical and electrical properties were observed.

3. Results and discussions

3.1. ZnO nanoparticles' structural properties

The prepared Aloe Vera Extract ZnO nanoparticles defined X-ray diffraction (XRD) pattern for crystal phases. Fig. 1 displays the XRD sequence of prepared ZnO nanoparticles displaying respectively the lattice planes (100), (002), (101), (102), (110), (103), (112), (201). The reported reflection of diffraction corresponded well to regular card no JCPDS 36-145 with a hexagonal wurtzite structure.

The size of the grain was determined by the Scherrer's method

$$D = \frac{K\lambda}{\beta \cos 6} \tag{1}$$

where D is crystalline, K is constant, i.e., 0.92 nm, β is half the maximum width, β is half the radius of the angle of Bragg. The crystal size has dropped between 20 and 30 nm. Illustration 1 notes that more peaks have been observed in the Zn nitrate hexahydrate than in the Zn acetate dehydrate.

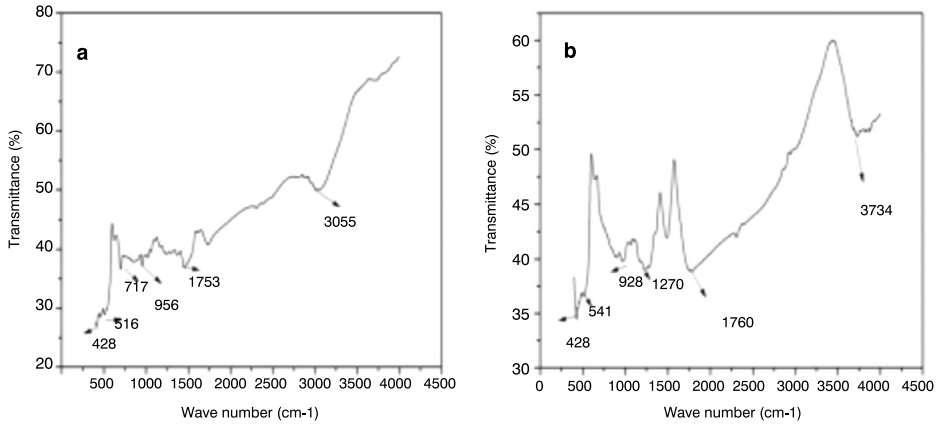

Fig. 3. FTIR spectra of Zn acetate and Zn nitrate with Aloe Vera extract.

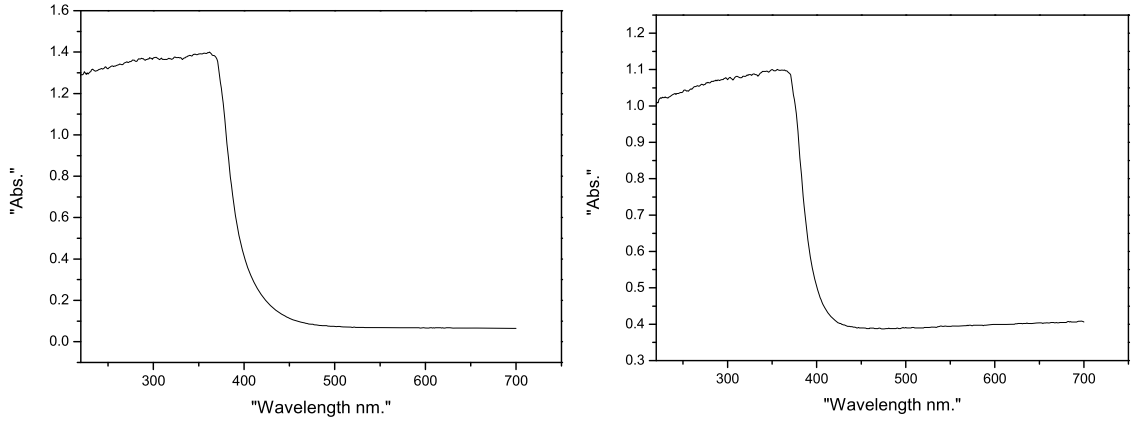

Fig. 4. Absorbance spectra of Zn acetate dehydrate and Zn nitrate hexahydrate.

Table 1
FTIR Spectra with the different synthesized ZnO based Nanoparticles.

Bond	Range $(cm)^{-1}$
OH	3500 – 4000
O=C=O	2330 – 2350
COO	1400 – 1750
ZnO	400 – 500

3.2. Morphological properties of ZnO nanoparticles

The overall morphology of aloe vera extract ZnO nanoparticles was analyzed using an electron microscope for field emission scanning (FESEM JEOL-JSM 6100). Fig. 2 (a) shows a rugged surface morphology while, in the case of ZnO nanoparticles synthesized with Zn nitrate hexahydrate as a parent solvent, simply nanoparticles have been produced. This rod-shaped and spherical design is also useful for the further application of photocatalytic and gas sensing. The average size of nanoparticles lies within the 40-50 nm band. It is the agreement with the results of the XRD which verified the best structure with peak diffraction.

3.3. Chemical composition of aloe vera extract ZnO nanoparticles

The KBr pallets by using FTIR spectrum is used to determine chemical composition of the samples. KBr's simple function is that it is inert, so it does not interfere with any other materials. Various peaks in FTIR spectra in the scale of 4000-400 cm^{-1} were observed in Fig. 3. Table 1 represents FTIR spectra bonds lies in the different ranges. Different functional community from the multiple peaks is examined. The band around the 3500-4000 cm^{-1} range is attributable to the OH community alone. The band is around 2330-2350 cm^{-1} can be due to the stretching O=C=O. The band near 1400-1750 cm^{-1} shows the group COO, and the band between 400-500 cm^{-1} shows the phase of ZnO stretching. ZnO is therefore up-to-date.

3.4. Optical properties

The optical properties of ZnO nanoparticles from the UV-Vis spectrophotometer have been characterized. The absorbance spectra were calculated in the range of 200-900 nm for these nanoparticles. Fig. 4 represents the highest absorption spectrum from 350-380 nm. The transmission spectrum can be derived via the following relationships from absorption spectra

$$\text{Absorbance} = 2 - \log_{10} T\,(\%) \tag{2}$$

Coefficients of direct transitional semiconductor absorption in relation to the optical band gap using the following equation

$$\alpha h\nu = A(h\nu - E_g)^n$$

Whilst the energy is hv, the optical band gap is E_g and the direct gap is n = 1/2, the indirect gap is n = 2 and the ZnO is the one with the direct band gap of n type semiconductor [18]. Fig. 5 shows linear plot of graph $(\alpha h\nu)^2$ and hv showed the optical band gap for ZnO nanoparticles in Fig. 7. The band gap of ZnO nanoparticles has been found to be in the range 3.10-3.20 eV. Table 2 represents band gap and refractive index of the different synthesized samples.

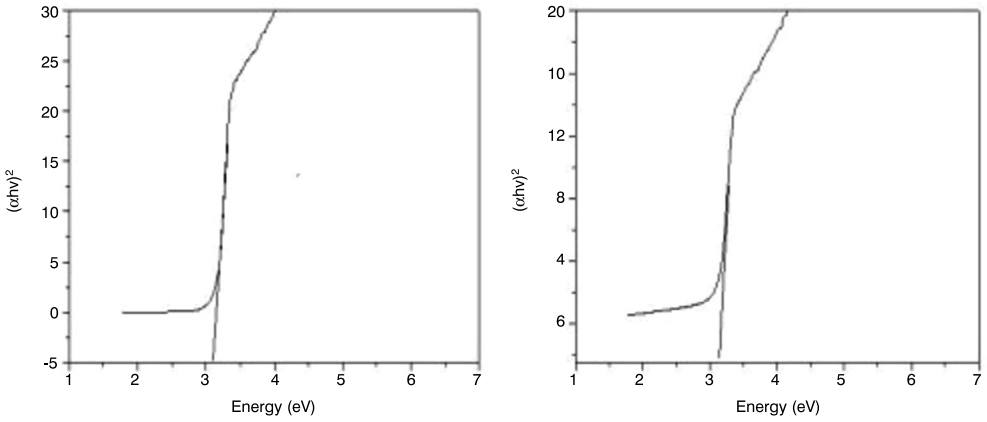

Fig. 5. A plot of $(\alpha hv)^2$ versus energy (eV) of ZnO nanoparticles.

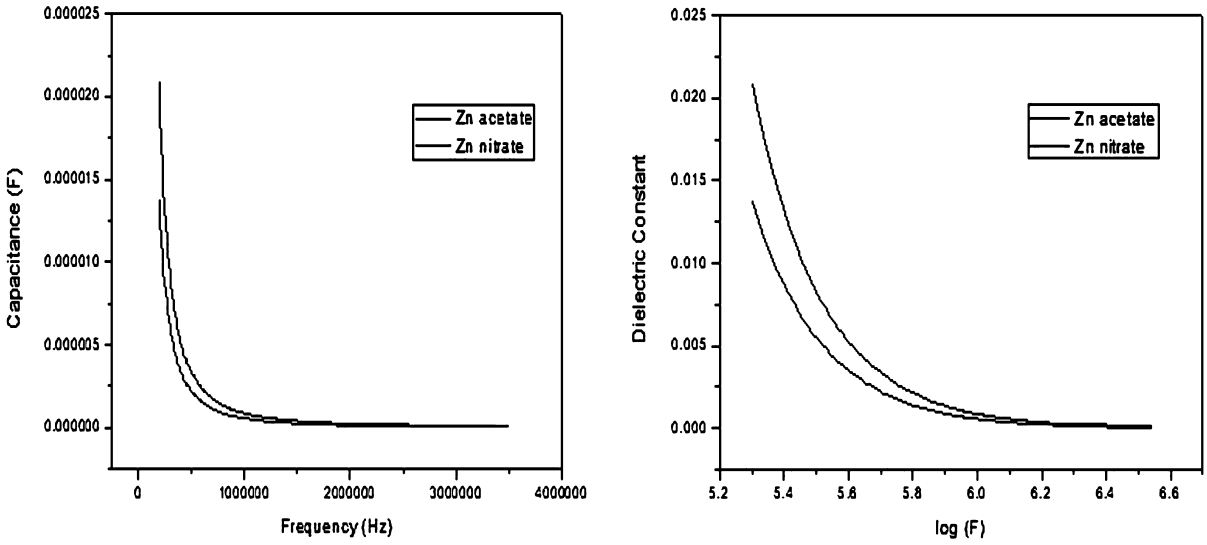

Fig. 6. Variation of capacitance with frequency of ZnO nanoparticles and variation of dielectric constant with frequency of ZnO nanoparticle.

Table 2
Band gap and refractive index of the synthesized sample by using different precursor.

Synthesized sample	Bandgap (eV)	Refractive index
Zn Acetate	3.10	2.00
Zn Nitrate	3.12	2.02

The ZnO nanoparticles refractive index can be calculated using the formulation

$$\frac{(n^2-1)}{(n^2+1)} = 1 - \frac{\sqrt{E_g}}{20} \tag{3}$$

In the range 2.00-2.02 of that formula the refractive index was found [19,20]. This corresponds approximately to the exact ZnO value. It was obtained from the above formula from the refractive index value.

3.5. Electrical properties

Some of the most significant and efficient approaches to research the variability in source solution of ZnO nanoparticles is the analysis of Capacity as a feature of operating frequency. Fig. 6 shows the variance of capacitance and dielectric constant with ZnO nanoparticles frequency and noticed that the capacitance value is small at a higher frequency. That is why ZnO nanoparticles can obey the ac signal [21] because of the high capacitance resulting from interface states in balance with aloe vera extract. The dielectric significance can be included in the formula

$$C = (\epsilon_0 \epsilon_r A)/d \tag{4}$$

Where C is capacitance, ϵ_0 is dielectric constant, A is the spherical pellet region and d is the thickness thereof. From Fig. 7 the dielectric constant was found to decrease with frequency. This difference in duration is attributed to relaxing time in transport [22].

Fig. 7 shows the variation between resistivity with applied frequency (0.2 MHz-3.5 MHz) of ZnO nanoparticles. The resistivity of different precursors with extract aloe vera is found to be frequency dependent which increases with applied frequency. The resistivity of ZnO nanoparticles lies in the range of 3.0-5.0 $\times 10^{-2}$ $(\Omega\,cm)^{-1}$. More resistivity is observed in case of Zn acetate as compared to Zn nitrate. This may be due to Z interstitial and oxygen vacancies [23,24].

4. Conclusions

In conclusion, using easy heat treatment process, specific source material with extract aloe vera ZnO nanoparticles was prepared and their effect on structural, morphological, optical and electrical properties was studied. XRD showed the nanometer-ordered polycrystalline structure of crystal dimension. Surface morphology

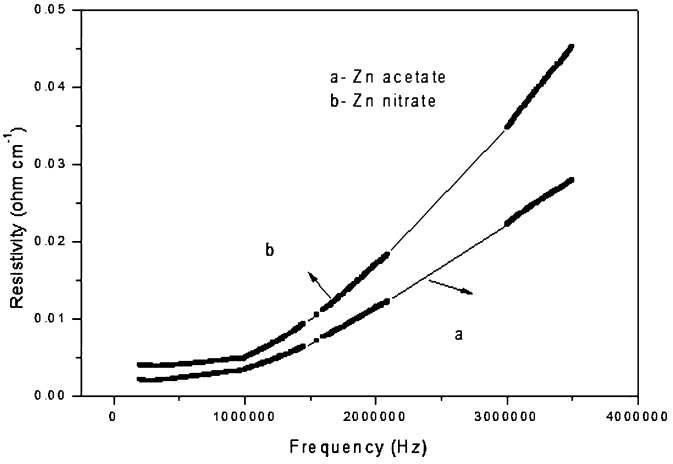

Fig. 7. Variation of resistivity with frequency of ZnO nanoparticles.

grain size is in line with XRD test. The difference in the optical band falls between 3.10-3.20 eV. The spectrum of resistivity is 3.0×10^{-2}–5.0×10^{-2} (average cm)$^{-1}$. The electrical properties study verified that such nanoparticles can be used for specific optoelectronic applications such as solar cell and gas sensor. These synthesized nanoparticles are further used for the fabrication of nanodevices which are further used for the medical purpose like in the neuroscience.

Declaration of competing interest

There is no conflict of interest.

References

[1] J. Qi, H. Zhang, S. Lu, et al., High performance indium-doped ZnO gas sensor, J. Nanomater. (2015), https://doi.org/10.1155/2015/954747.
[2] N. Srinatha, Y.S. No, V.B. Kamble, et al., Effect of RF power on the structural, optical and gas sensing properties of RF-sputtered Al doped ZnO thin films, RSC Adv. 6 (2016) 9779–9788, https://doi.org/10.1039/C5RA22795J.
[3] R.K. Nath, S.S. Nath, K. Sunar, Sn-doped zinc oxide thin films for LPG sensors, J. Anal. Sci. Technol. 3 (2012) 85–94, https://doi.org/10.5355/JAST.2012.85.
[4] Y. Hsiou, W. Hung, C. Wang, Fabrication of Sb-doped p-type ZnO thin films by pulsed laser deposition, Atlas J. Mater. Sci. 2 (2015) 60–64, https://doi.org/10.5147/ajms.2015.0166.
[5] K. Raja, P.S. Ramesh, D. Geetha, Synthesis, structural and optical properties of ZnO and Ni-doped ZnO hexagonal nanorods by Co-precipitation method, Spectrochim. Acta, Part A, Mol. Biomol. Spectrosc. 120 (2014) 19–24, https://doi.org/10.1016/j.saa.2013.09.103.
[6] S. Bhatia, N. Verma, R.K. Bedi, Optical application of Er-doped ZnO nanoparticles for photodegradation of direct red - 31 dye, Opt. Mater. 62 (2016) 392–398, https://doi.org/10.1016/j.optmat.2016.10.013.
[7] S. Bhatia, N. Verma, Erbium-doped nanoparticles/films for enhancing percentage photodegradation of direct red-31 dye, J. Mater. Sci., Mater. Electron. (0 2018) 1–11, https://doi.org/10.1007/s10854-018-9634-7.
[8] A. Khataee, R. Darvishi, C. Soltani, et al., Synthesis and Characterization of Dysprosium-Doped ZnO Nanoparticles for Photocatalysis of a Textile Dye Under Visible Light Irradiation, 2014.
[9] D. Liu, Y. Liu, Z. Wu, et al., By microwave radiation with visible light response for naphthalene, J. Chin. Inst. Chem. Eng. (0 2016) 1–8, https://doi.org/10.1016/j.jtice.2016.10.002.
[10] P. Activities, K. Han, X. Peng, et al., SnO_2 composite films for enhanced, Catalysis (2018) 1–12, https://doi.org/10.3390/catal8100453.
[11] A. Seetharaman, A. Nithya, K. Jothivnkatachalam, Three way electron transfer of C-N-S tri doped two-phase junction of TiO_2 nanoparticles for efficient visible light photocatalytic dye degradation, https://doi.org/10.1039/C5RA25017J, 2016.
[12] S. Bhatia, N. Verma, Gas sensing performance of dip-coated indium-doped ZnO films, J. Electron. Mater. (2018), https://doi.org/10.1007/s11664-018-6533-x.
[13] M. Rakhra, R. Singh, T.K. Lohani, M. Shabaz, Metaheuristic and machine learning-based smart engine for renting and sharing of agriculture equipment, 2021, 2021.
[14] S. Sarahnaz, O.P. Gujela, N.V. Afzulpurkar, in: Fabrication of Light Emitting Diode with ZnO Nanorods on Polymer Coated Silicon Substrate, 2013, pp. 295–298.
[15] F. Li, L. Orosz, O. Kamoun, et al., ZnO-based polariton laser operating at room temperature: from excitonic to photonic condensate, Condens. Matter (2012), https://doi.org/10.1103/PhysRevLett.110.196406.
[16] S. Bhatia, N. Verma, R.K. Bedi, Results in physics ethanol gas sensor based upon ZnO nanoparticles prepared by different techniques, Results Phys. 7 (2017) 801–806, https://doi.org/10.1016/j.rinp.2017.02.008.
[17] C. Zegadi, K. Abdelkebir, D. Chaumont, et al., Influence of Sn low doping on the morphological, structural and optical properties of ZnO films deposited by sol gel dip-coating, Adv. Mater. Phys. Chem. 04 (2014) 93–104, https://doi.org/10.4236/ampc.2014.45012.
[18] G. Singh, S.B. Shrivastava, D. Jain, et al., Effect of indium doping on zinc oxide films prepared by chemical spray pyrolysis technique, Bull. Mater. Sci. 33 (2010) 581–587.
[19] S.D. Senol, Hydrothermal derived nanostructure rare earth (Er, Yb)-doped ZnO: structural, optical and electrical properties, J. Mater. Sci., Mater. Electron. 27 (2016) 7767–7775, https://doi.org/10.1007/s10854-016-4765-1.
[20] M. Rakhra, N. Verma, Tri-doped co-annealed zinc oxide semi-conductor synthesis and characterization: photodegradation of dyes and gas sensing applications, J. Mater. Sci., Mater. Electron. (2021), https://doi.org/10.1007/s10854-021-06292-9.
[21] B. Zhau, F. Wang, Chen H. et al, An ultrahigh responsivity (9.7 mA W−1) self-powered solar-blind photodetector based on individual ZnO–Ga_2O_3 heterostructures, Adv. Funct. Mater. 27 (2017) 1700264.
[22] W. Sinornate, H. Mimmura, W. Pecharapa, Structural, morphological, optical, and electrical properties of sol–gel derived Sb-doped ZnO thin films annealed under different atmospheres, https://doi.org/10.1002/pssa.202000233, 2020.
[23] M. Rakhra, N. Verma, S. Bhatia, Structural, morphological, optical, electrical and agricultural properties of solvent / ZnO nanoparticles in the photodegradation of DR-23 dye, https://doi.org/10.1007/s11664-019-07760-z, 2019.
[24] A. Tabib, W. Bouslama, B. Sieber, A. Addad, H. Elhouichet, M. Férid, R. Boukherroub, Structural and optical properties of Na doped ZnO nanocrystals: application to solar photocatalysis, Appl. Surf. Sci. 396 (2017) 1528–1538, https://doi.org/10.1016/j.apsusc.2016.11.204.